NANJING INSTITUTE OF GEOPHYSICAL PROSPECTING AND INSTITUTE OF PHYSICS PUBLISHING — JOURNAL OF GEOPHYSICS AND ENGINEERING

J. Geophys. Eng. 1 (2004) 234–239 — PII: S1742-2132(04)79784-8

# Effects of clay content and porosity on wave velocities in unconsolidated media using empirical relations

**J A Olowofela[1], I C Kamiyole[2] and J A Adegoke[1]**

[1] Department of Physics, University of Ibadan, Ibadan, Nigeria
[2] Department of Physics, Oyo-State College of Education, Oyo, Nigeria

Received 20 April 2004
Accepted for publication 16 July 2004
Published 24 August 2004
Online at stacks.iop.org/JGE/1/234
doi:10.1088/1742-2132/1/3/009

**Abstract**
Wave velocities in sandstones are greatly influenced by porosity and clay contents. We formulated new empirical relations for the velocities $V_p$ and $V_s$ in these media which take into account the porosity and clay contents. These relations are $V_p = 5.57 - 6.47\phi - 2.27C^{1-\phi}$ and $V_s = 3.41 - 4.44\phi - 2.23C^{1-\phi}$, and can be used to compute velocities for various porosities and clay contents. The results compare favourably with those of other works.

**Keywords:** Porosity, clay content, wave velocity, unconsolidated media



## 1. Introduction

Most igneous and metamorphic rocks have little or no porosity and velocities of seismic waves in such rocks depend mainly on the elastic properties of their constituent minerals. In general, velocities of seismic waves in igneous rocks show a narrower range of variation than those in sedimentary or metamorphic rocks. The average velocity in igneous rocks is higher than that in other types of rocks. The rock with the highest velocities is dunite—an ultrabasic rock that some believe is an important constituent of the earth's mantle. Most metamorphic rocks show an even wider range of variation in velocity, e.g., in gneiss, velocities range from 3536 to 7559 $m\ s^{-1}$. Sedimentary rocks generally exhibit a much greater per cent increase in velocity with increasing pressure.

Seismic velocities are quite different in different sedimentary rocks. These rocks show little variation in speed even for different depths of burial. The highest reported velocity in sedimentary rocks is about 7620 $m\ s^{-1}$ in a dolomitic limestone. The key to the variation appears to be density and porosity.

In most sedimentary rocks, the actual velocity is dependent on the intrinsic velocity in the minerals constituting the solid rock matrix, the porosity, the pore pressure and the velocity in the fluid filling the pore spaces. It also depends on the composition of any solid cementing material between the grains of the primary rock constituents. At shallow depths of burial, the velocity in most sedimentary rocks increases rapidly with increasing pressure. For rocks with grains that are approximately spherical, a theoretical relationship was developed by Gassmann which predicts that the velocity should be proportional to the pressure raised to the one-sixth power, and the constant of proportionality is expressed in terms of the elastic constant and density of the rock material itself. Beyond the depth where such consolidation is reached, the influence of variation in pressure on velocity becomes small, and therefore the porosity and mineral composition of the grains become dominant in governing velocity. A very simple linear relationship between the reciprocal of the velocity and porosity has been found by Wyllie *et al* (1956) for a water-saturated sandstone at depths greater than a few thousand feet.

$$\frac{1}{V} = \frac{\phi}{V_F} + \frac{1-\phi}{V_m} \qquad (1)$$

where $V$ is the velocity in saturated rock, $\phi$ is the fractional porosity, $V_F$ is the velocity of fluid in the pore space and $V_m$ is the velocity of solid material making up the rock matrix. Equation (1) is known as the time-averaged relationship. Where it holds, the velocity $V$ would be equal to $V_m$ at zero porosity and to $V_F$ at 100% porosity, its reciprocal $\frac{1}{V}$ being linearly related to $\phi$ for values inbetween. The observed velocities for sandstones show a very close adherence to the time-average relationship over the porosity range between zero and 30%.

A similar equation developed from theoretical considerations by Pickett (1969) is

$$\frac{1}{V} = A + B\phi, \tag{2}$$

where $A$ and $B$ depend on lithologic parameters and depths of burial. Equation (2) appears to be valid for a wider range of sedimentary rocks.

## 2. Wave velocities in sandstones from elastic network simulations

The elastic wave velocities in rocks are difficult to calculate just from knowledge of the composition and microstructure. An elastic network model provides a framework for quantitative prediction of elastic wave velocities. The elastic network model uses a regular lattice of grains with elastic interactions between nearest neighbours. The grain-to-grain elastic interactions include the rotational motion of the individual grains in addition to the translational motion normal and parallel to the contact plane between grains (Schwartz *et al* 1984). The elastic network model consists of a three-dimensional network of grains, with each grain connected to its neighbours by springs. The stiffness of the springs represents the amount of cementation and grain-to-grain contact between neighbouring grains (Curtin and Scher 1990, Limat 1989).

The implementation of the elastic network model differs from the work of Schwartz *et al* (1984) in its treatment of porosity. In the model, solid grains are distributed on a regular lattice. All lattice sites are occupied by grains with porosity defined as the void spaces between grains, but in the elastic network model, each lattice site represents an element of volume that can be either solid grain or pore. Porosity is created by the remaining solid grains from the lattice site, and porosity in the elastic network model is defined as the fraction of empty lattice sites. The advantage of this definition of porosity is that the spring constants describing elastic interactions between neighbouring grains can be treated as constants independent of porosity. The model provides a microscopic foundation for the use of a linear velocity–porosity relationship. Calculations using the model predict a linear dependence of the compressional velocity on both water-saturated porosity and the total clay content. The network model provides an alternative to the Biot theory for calculating velocities in fluid-saturated media (Biot 1956a, 1956b). The Biot theory requires the acoustic properties of the dry porous medium (also called the dry frame) as input, which are used to predict the fluid-saturated properties. The elastic network model can be used to calculate the dry frame acoustic properties of the fluid-saturated medium without separate knowledge of the dry frame.

A porous sandstone composed of various minerals can be modelled by varying the spring constants between neighbouring grains to reflect the different elastic properties of the rock constituents. The elastic properties of the entire network can be calculated from the set of all spring constants between neighbouring grains. The simulations are limited to cubic lattices, where each lattice site has six bonds to neighbouring sites.

The elastic interaction between neighbouring grains is described by a potential energy that depends on the displacement of the grains away from their equilibrium positions. For the special case in which the two grains $i$ and $j$ are confined to move in only one dimension, the potential energy is found from Hooke's law as

$$V_{ij} = \tfrac{1}{2}KU_{ij}^2 \tag{3}$$

where $U_{ij}$ is the displacement of the grains relative to their equilibrium position and $K$ is a spring constant. In three dimension, the potential energy depends on both a vector relative displacement $U_{ij}$ and the angles of rotation from equilibrium $\theta_i$ and $\theta_j$ at each grain. Schwartz *et al* (1984, 1985) and Feng (1985) developed the full 3D case including rotations. Neighbouring grains are connected by three springs with spring constants $K_{11}$, $k_\perp$ and $K_\gamma$, respectively. The potential energy is

$$V_{ij} = \tfrac{1}{2}K_{11}(U_{ij}\cdot\hat{r}_{ij})^2 + \tfrac{1}{2}K_\perp[(U_{ij}\times\hat{r}_{ij})\hat{r}_{ij} + R(\theta_i+\theta_j)\times\hat{r}_{ij}]^2 + \tfrac{1}{2}K_\gamma^2(\theta_i-\theta_j)^2 \tag{4}$$

where $\hat{r}_{ij}$ is the unit vector between neighbouring grains $i$ and $j$, and $R$ is the grain radius.

The first term in equation (4) is the central force term and it accounts for the restoring force along a line connecting two nearest-neighbour grains. The second term opposes the displacement of the contact point perpendicular to a line connecting the two grains or from a rotation where both grains rotate in the same direction, without movement of the grains' centre. The third term opposes counter-rotation where the grains rotate in opposite directions with no relative displacements.

Schwartz *et al* (1984) showed that in an elastic network model without rotation, it is possible to have an infinite Poisson ratio. When the rotational terms are included, the models with and without rotational terms behave differently near the percolation threshold (Alexander 1984, Kantour and Webman 1984). This means that the rotational terms are particularly important for simulation at high porosities. The presence of a third spring constant in the expression for the energy of interactions implies the existence of a third vibrational mode in the network in addition to the usual compressional and shear modes.

The P-wave velocity $V_p$ from the network simulation (Gist *et al* 1993) as a function of water-saturated porosity $\phi$ is given by

$$V_p = 5.45 - 6.17\phi, \tag{5}$$

$$V_s = 3.59 - 5.50\phi. \tag{6}$$

Han *et al* (1986) set up an experiment in which expressions for both P-wave velocity $V_p$ and S-wave velocity $V_s$ were obtained. They fit $V_p$ measured at a confining pressure of 40 MPa to a linear function of both porosity and clay content. When the clay content was set to zero, in their best-fit equation, the expressions for $V_p$ and $V_s$ of clay-free sandstones are given by

$$V_p = 5.59 - 6.93\phi, \quad \text{and} \tag{7}$$

**Table 1.** Parameter for $V_p$.

| Method | $A_0$ | $A_1$ | $A_2$ |
|---|---|---|---|
| Network simulation[a] | 5.30 | 6.00 | 2.43 |
| Ultrasonic core tests[a] | 5.59 | 6.93 | 2.18 |
| Frio formation[b] | 5.81 | 9.42 | 2.21 |
| Empirical relations[c] | 5.57 | 6.47 | 2.27 |

[a] Han *et al* (1986).
[b] Castagna *et al* (1985).
[c] New empirical relation.

**Table 2.** Parameter for $V_s$.

| Method | $B_0$ | $B_1$ | $B_2$ |
|---|---|---|---|
| Network simulation[a] | 3.29 | 3.97 | 2.39 |
| Ultrasonic core tests[a] | 3.52 | 4.91 | 1.89 |
| Frio formation[b] | 3.89 | 7.07 | 2.04 |
| Empirical relations[c] | 3.41 | 4.44 | 2.23 |

[a] Han *et al* (1986).
[b] Castagna *et al* (1985).
[c] New empirical relation.

**Table 3.** Computation of $V_p$ using different methods.

| $\phi$ | Clay content | NS $V_p$ (km s$^{-1}$) | UCT $V_p$ (km s$^{-1}$) | FF $V_p$ (km s$^{-1}$) | ER $V_p$ (km s$^{-1}$) |
|---|---|---|---|---|---|
| 0.1 | 0.2 | 4.214 | 4.461 | 4.426 | 4.389 |
| 0.2 | 0.2 | 3.614 | 3.768 | 3.484 | 3.65 |
| 0.3 | 0.2 | 3.014 | 3.075 | 2.545 | 2.89 |
| 0.4 | 0.2 | 2.414 | 2.382 | 1.600 | 2.12 |
| 0.5 | 0.2 | 1.814 | 1.689 | 0.658 | 1.32 |

Using $V = A_0 - A_1\phi - A_2C$ and $V = A_0 - A_1\phi - A_2C^{1-\phi}$ (for the empirical relation). NS: network simulation; UCT: ultra core test; FF: frio formation; ER: empirical relation.

**Table 4.** Computation of $V_s$ using different methods.

| $\phi$ | Clay content | NS $V_s$ (km s$^{-1}$) | UCT $V_s$ (km s$^{-1}$) | FF $V_s$ (km s$^{-1}$) | ER $V_s$ (km s$^{-1}$) |
|---|---|---|---|---|---|
| 0.1 | 0.2 | 2.415 | 2.651 | 2.775 | 2.4421 |
| 0.2 | 0.2 | 2.018 | 2.160 | 2.068 | 1.9067 |
| 0.3 | 0.2 | 1.621 | 1.669 | 1.361 | 1.3552 |
| 0.4 | 0.2 | 1.224 | 1.178 | 0.654 | 0.785 |
| 0.5 | 0.2 | 0.827 | 0.687 | −0.053[a] | 0.7428 |

[a] Unrealistic value.

**Table 5.** Computation of $V_p/V_s$ using different methods.

| | Clay content | NS $V_p/V_s$ | UCT $V_p/V_s$ | FF $V_p/V_s$ | ER $V_p/V_s$ |
|---|---|---|---|---|---|
| 0.1 | 0.2 | 1.744 | 2.12 | 1.59 | 1.80 |
| 0.2 | 0.2 | 1.79 | 1.673 | 1.685 | 1.91 |
| 0.3 | 0.2 | 1.86 | 1.81 | 1.87 | 2.13 |
| 0.4 | 0.2 | 1.97 | 2.02 | 2.45 | 2.70 |
| 0.5 | 0.2 | 2.19 | 2.46 | [a] | 1.77 |

[a] Unrealistic value.

$$V_s = 3.60 - 5.53\phi, \tag{8}$$

respectively.

Averaging the resulting expressions from Gist *et al* (1993) and Han *et al* (1986) leads to the new empirical relations:

$$V_p = 5.52 - 6.55\phi, \tag{9}$$

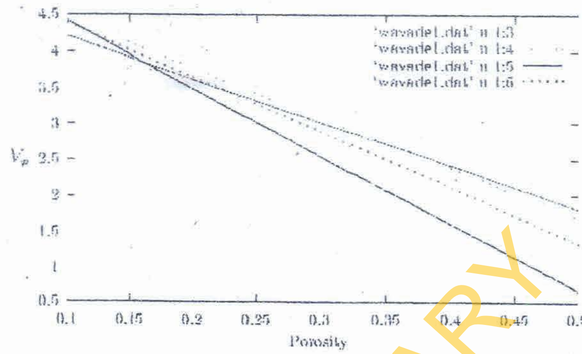


**Figure 1.** A plot of $V_p$ versus porosity with clay content 0.2 where 'wavade1.dat' u 1:6 is the new empirical relation.

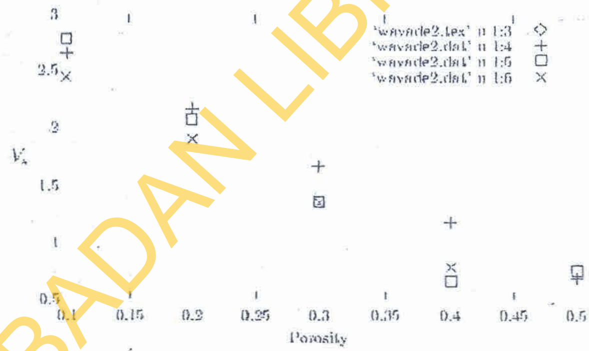


**Figure 2.** A plot of $V_s$ versus porosity with clay content 0.2 where 'wavade2.dat' u 1:6 is the new empirical relation.

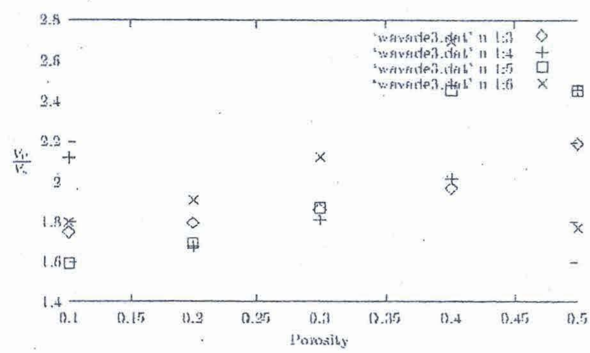


**Figure 3.** A plot of $V_p/V_s$ versus porosity with clay content 0.2 where 'wavade3.dat' u 1:6 is the new empirical relation.

and

$$V_s = 3.49 - 5.12\phi. \tag{10}$$

*2.1. Dependence of velocity on porosity and clay content*

The linear dependence of P-wave velocity ($V_p$) on both porosity and clay content, combined with the change in velocity with clay content at different porosities, implies that the velocity from the simulations can be written as a bilinear

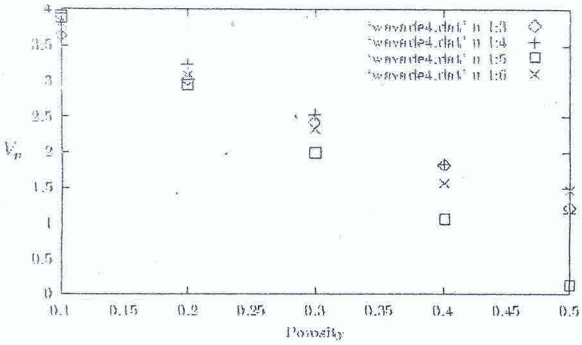


**Figure 4.** A plot of $V_p$ versus porosity with clay content 0.4472 where 'wavade4.dat' u 1:6 is the new empirical relation.

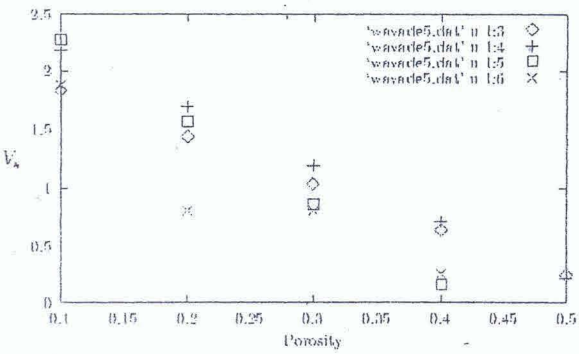


**Figure 5.** A plot of $V_s$ versus porosity with clay content 0.4472 where 'wavade5.dat' u 1:6 is the new empirical relation.

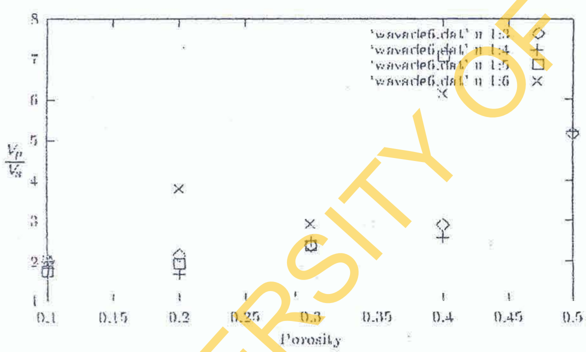


**Figure 6.** A plot of $V_p/V_s$ versus porosity with clay content 0.4472 where 'wavade6.dat' u 1:6 is the new empirical relation.

**Table 6.** Computation of $V_p$ using different methods and different values of clay content.

| $\phi$ | Clay content | NS $V_p$ (km s$^{-1}$) | UCT $V_p$ (km s$^{-1}$) | FF $V_p$ (km s$^{-1}$) | ER $V_p$ (km s$^{-1}$) |
|---|---|---|---|---|---|
| 0.1 | 0.4472 | 3.6133 | 3.9221 | 3.8797 | 3.8228 |
| 0.2 | 0.4472 | 3.0133 | 3.2291 | 2.9377 | 3.0836 |
| 0.3 | 0.4472 | 2.4133 | 2.5361 | 1.9957 | 2.3367 |
| 0.4 | 0.4472 | 1.8133 | 1.8431 | 1.0537 | 1.5814 |
| 0.5 | 0.4472 | 1.2133 | 1.1501 | 0.117 | 1.464 |

function in porosity and clay content:

$$V = A_0 - A_1\phi - A_2\phi. \quad (11)$$

**Table 7.** Computation of $V_s$ using different methods and different values of clay content.

| $\phi$ | Clay content | NS $V_s$ (km s$^{-1}$) | UCT $V_s$ (km s$^{-1}$) | FF $V_s$ (km s$^{-1}$) | ER $V_s$ (km s$^{-1}$) |
|---|---|---|---|---|---|
| 0.1 | 0.4472 | 1.8242 | 2.1838 | 2.2707 | 1.885 |
| 0.2 | 0.4472 | 1.4272 | 1.6928 | 1.5637 | 0.808 |
| 0.3 | 0.4472 | 1.0302 | 1.2018 | 0.8567 | 0.8084 |
| 0.4 | 0.4472 | 0.6332 | 0.7108 | 0.1497 | 0.258 |
| 0.5 | 0.4472 | 0.2362 | 0.2198 | [a] | [a] |

[a] Unrealistic value.

**Table 8.** Computation of $V_p/V_s$ using different methods and different values of clay content.

| $\phi$ | Clay content | NS $V_p/V_s$ | UCT $V_p/V_s$ | FF $V_p/V_s$ | ER $V_p/V_s$ |
|---|---|---|---|---|---|
| 0.1 | 0.4472 | 1.98 | 1.80 | 1.71 | 2.02 |
| 0.2 | 0.4472 | 2.11 | 1.67 | 1.88 | 3.82 |
| 0.3 | 0.4472 | 2.34 | 2.46 | 2.33 | 2.89 |
| 0.4 | 0.4472 | 2.86 | 2.59 | 7.04 | 6.13 |
| 0.5 | 0.4472 | 5.14 | 5.23 | [a] | [a] |

[a] Unrealistic value.

**Table 9.** Computation of $V_p$ with values of clay content varying from 0.1 to 0.5 at different porosities.

| Clay content | $\phi = 0.1$ | $\phi = 0.2$ | $\phi = 0.3$ | $\phi = 0.4$ | $\phi = 0.5$ |
|---|---|---|---|---|---|
| 0.1 | 4.637 224 | 3.916 229 | 3.176 075 | 2.411 802 | 1.617 163 |
| 0.2 | 4.389 723 | 3.649 603 | 2.893 222 | 2.117 741 | 1.319 825 |
| 0.3 | 4.154 87 | 3.409 591 | 2.651 739 | 1.879 703 | 1.091 67 |
| 0.4 | 3.927 87 | 3.185 379 | 2.433 725 | 1.672 028 | 0.899 326 |
| 0.5 | 3.706 537 | 2.972 227 | 2.231 651 | 1.484 359 | 0.729 868 |

**Table 10.** Computation of $V_s$ with values of clay content varying from 0.1 to 0.5 at different porosities.

| Clay content | $\phi = 0.1$ | $\phi = 0.2$ | $\phi = 0.3$ | $\phi = 0.4$ | $\phi = 0.5$ |
|---|---|---|---|---|---|
| 0.1 | 2.685 26 | 2.168 569 | 1.633 057 | 1.073 849 | 0.484 812 |
| 0.2 | 2.442 12 | 1.906 641 | 1.355 187 | 0.784 97 | 0.192 714 |
| 0.3 | 2.211 405 | 1.670 858 | 1.117 959 | 0.551 127 | −0.031 421 |
| 0.4 | 1.988 405 | 1.450 597 | 0.903 787 | 0.347 112 | −0.220 376 |
| 0.5 | 1.770 973 | 1.241 201 | 0.705 274 | 0.162 749 | −0.386 848 |

**Table 11.** Computation of $V_s/V_p$ with values of clay content varying from 0.1 to 0.5 at different porosities.

| Clay content | $\phi = 0.1$ | $\phi = 0.2$ | $\phi = 0.3$ |
|---|---|---|---|
| 0.1 | 1.726 918 | 1.805 905 | 1.944 866 |
| 0.2 | 1.797 505 | 1.914 154 | 2.134 924 |
| 0.3 | 1.878 837 | 2.040 623 | 2.371 946 |
| 0.4 | 1.975 387 | 2.195 909 | 2.692 808 |
| 0.5 | 2.092 939 | 2.394 638 | 3.164 233 |

This equation was used by Han *et al* (1986) to fit ultrasonic compressional and shear velocities to porosity and clay content, and by Castagna *et al* (1985) in analysing sonic logs in shaly sandstones. Han *et al* (1986) show that equation (11)

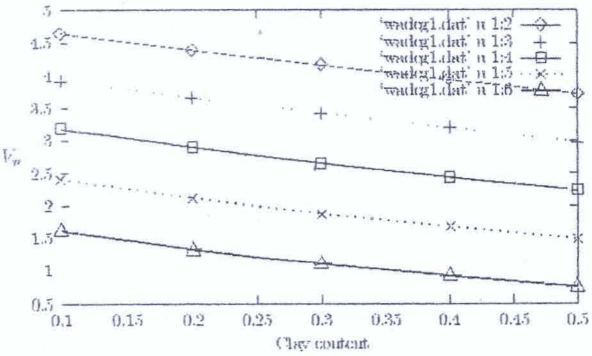


**Figure 7.** A plot of $V_p$ versus clay content which varies from 0.1 to 0.5 for the new empirical relation. 'wadcg1.dat' u 1:2→ $\phi = 0.1$, 'wadcg1.dat' u 1:3 → $\phi = 0.2$, 'wadcg1.dat' u 1:4→ $\phi = 0.3$, 'wadcg1.dat' u 1:5 → $\phi = 0.4$, 'wadcg1.dat' u 1:6→ $\phi = 0.5$.

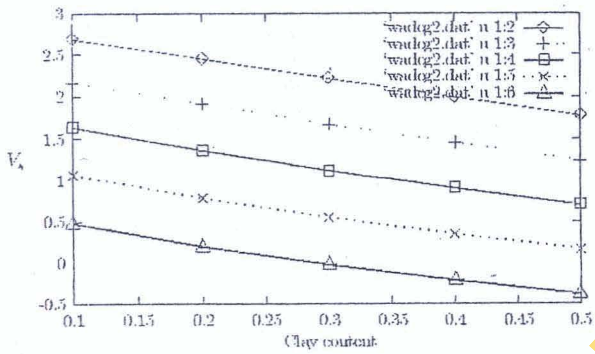


**Figure 8.** A plot of $V_s$ versus clay content which varies from 0.1 to 0.5 for the new empirical relation. 'wadcg2.dat' u 1:2→ $\phi = 0.1$, 'wadcg2.dat' u 1:3 → $\phi = 0.2$, 'wadcg2.dat' u 1:4→ $\phi = 0.3$, 'wadcg2.dat' u 1:5 → $\phi = 0.4$, 'wadcg2.dat' u 1:6→ $\phi = 0.5$.

gives a better fit to the experimental data than the modified Wyllie time average

$$\frac{1}{V} = B_0 - B_1\phi - B_2\phi. \qquad (12)$$

Network simulation data were analysed in the same manner. Han *et al* (1986) modified their experimental data by fitting the simulation results to equations (11) and (12).

A third velocity–porosity clay equation introduced by Eberhart-Phillips *et al* (1989) replaces the linear dependence of velocity on clay content with the square root of the clay content:

$$V = B_0 - D_1\phi - D_2\phi. \qquad (13)$$

They claimed a significant improvement in the fit to ultrasonic data using equation (13) compared to the linear clay term of equation (11). Generally speaking

$$V = A_0 - A_1\phi - A_2C. \qquad (14)$$

$$V = B_0 - B_1\phi - B_2\phi. \qquad (15)$$

The values of constants $A_0$, $A_1$, $A_2$, $B_0$, $B_1$ and $B_2$ are given in tables 1 and 2. However, the new empirical relations are given by

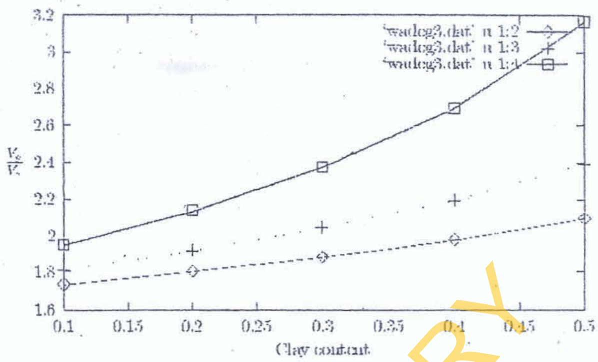


**Figure 9.** A plot of $V_s$ versus clay content which varies from 0.1 to 0.5 for the new empirical relation. 'wadcg3.dat' u 1:2→ $\phi = 0.1$, 'wadcg3.dat' u 1:3 → $\phi = 0.2$, 'wadcg3.dat' u 1:4→ $\phi = 0.3$

$$V_p = 5.57 - 6.47\phi - 2.27C^{1-\phi} \qquad (16)$$

$$V_s = 3.41 - 4.44\phi - 2.23C^{1-\phi}. \qquad (17)$$

Values of the compressional wave velocity ($V_p$) and shear wave velocity ($V_s$) using equation (13), which is the Eberhart-Phillips equation, as a function of porosity and clay content using

$$V_p = B_0 - B_1\phi - B_2C^{1/2} \qquad (18)$$

$$V_s = D_0 - D_1\phi - D_2C^{1/2} \qquad (19)$$

have been reported. We used the newly formulated empirical relation to compute the velocities and compared them with the reported results (Han *et al* 1986).

## 3. Discussion

We compute new empirical relations with different experimental and theoretical results as shown in tables 3–9. Table 3 gives the computation of the velocity of P-waves, $V_p$, in the sandstones with the clay content 0.2. We also compute the velocity of S-waves, $V_s$, in the sandstones with clay content 0.2, as shown in table 5. Table 5 also shows the ratios of $V_p$ to $V_s$ with respect to porosity. From these tables one can clearly see that the results of the new empirical relations compare favourably with established experimental and other theoretical works. This is also demonstrated in figures 1–3.

Similarly, we carried out the same computation as given in tables 3–5 in tables 6–8 and we have plotted the corresponding graphs in figures 4–6.

Although the new empirical relation still holds for clay contents between 0.1 and 0.3, it suffers setback at clay contents 0.4 and 0.5 when porosity is 0.5.

This failure is not peculiar to this empirical relation, but it also affects the Frio formation, which leads to the investigation of the behaviour of the emprirical relation with clay content as shown in tables 9–11. The empirical relation clearly holds at porosities 0.1 to 0.5 provided the clay content is not greater than 0.3 (figures 7–9).

## 4. Conclusion

A new relationship has been found that can be used to easily determine the velocities of P- and S-waves in sandstones with some amount of clay. Although there is a limitation in using this expression when the clay content is close to 0.5, this is not a serious deficiency. Sandstones with 0.5 clay content cannot really be regarded as sandstones; they can just as well be described as clay with 0.5 sand content.

Hence in a typical sandstone region, where there is some clay content, these empirical relations are valid for any porosity provided that the clay content is not greater than 0.3. However, we found that the results might still be used where the clay content is in the neighbourhood of 0.4. It is safer to limit its use to the clay content 0.3 for any porosity of sandstone. Consequently, the new empirical relationships for $V_p$ and $V_s$ are valid for determining velocities of P- and S-waves in unconsolidated media.

## References


Alexander S 1984 Is the elastic energy of amorphous materials rotationally invariant? *J. Physique* **45** 1939–45

Biot M A 1956a Theory of propagation of elastic waves in a fluid-saturated porous solid: I. Low frequency range *J. Acoust. Soc. Am.* **28** 168

Biot M A 1956b Theory of propagation of elastic waves in a fluid-saturated porous solid: II. Higher frequency range *J. Acoust. Soc. Am.* **28** 168

Castagna J P, Batzle M I and Eastwood R J 1985 Relationships between compressional wave and shear wave velocities in clastic silicate rocks *Geophysics* **59** 571–81

Curtin W A and Scher H 1990 Brittle fracture in disordered materials: a spring network model *J. Mater. Res.* **5** 535–53

Eberhart-Phillips D, Hans D H and Zoback M D 1989 Empirical relationships among seismic velocity, effective pressure and clay contents in sandstones *Geophysics* **54** 82–9

Feng S 1985 Percolation properties of granular elastic networks in two dimensions *Phys. Rev. Lett.* **52** 216–9

Gist G A, Thompson A U and Berry M J II 1993 Wave velocities in sandstone from elastic network simulations *Geophysics* **58** 334–43

Han D, Nur A and Morgan F D 1986 Effects of porosity and clay content on wave velocities in sandstones *Geophysics* **52** 2093

Kantor Y and Webman I 1984 Elastic properties of random percolating systems *Phys. Rev. Lett.* **52** 1891–4

Limat L 1989 Elastic and superelastic percolation networks: imperfect duality, critical Poisson's ratios and relations between microscopic models *Phys. Rev.* B **40** 9253–68

Pickett G R 1969 Principle for application of borehole measurements in petroleum engineering *Log. Anal.* (May–June) 22–3

Shwartz L M, Feng S, Thorpe M F and Sen P N 1985 Behaviour of depleted elastic network: comparison of effective medium and numerical calculations *Phys. Rev.* B **32** 4607–17

Schwartz L M, Johnson D I and Feng S 1984 Vibrational modes in granular materials *Phys. Rev. Lett.* **52** 831–4

Wyllie M R J, Gregory A R and Gardner G H 1956 Elastic wave velocities in heterogeneous and porous media *Geophysics* **21** 41–70